Anal Bioanal Chem (2015) 407:2365–2371
DOI 10.1007/s00216-014-8012-4

RESEARCH PAPER

Quantitative bioimaging of *p*-boronophenylalanine in thin liver tissue sections as a tool for treatment planning in boron neutron capture therapy

Olga Reifschneider · Christian L. Schütz · Christoph Brochhausen · Gabriele Hampel · Tobias Ross · Michael Sperling · Uwe Karst

Received: 5 February 2014 / Revised: 12 June 2014 / Accepted: 30 June 2014 / Published online: 12 July 2014

Abstract An analytical method using laser ablation-inductively coupled plasma-mass spectrometry (LA-ICP-MS) was developed and applied to assess enrichment of ^{10}B-containing *p*-boronophenylalanine-fructose (BPA-f) and its pharmacokinetic distribution in human tissues after application for boron neutron capture therapy (BNCT). High spatial resolution (50 μm) and limits of detection in the low parts-per-billion range were achieved using a Nd:YAG laser of 213 nm wavelength. External calibration by means of ^{10}B-enriched standards based on whole blood proved to yield precise quantification results. Using this calibration method, quantification of ^{10}B in cancerous and healthy tissue was carried out. Additionally, the distribution of ^{11}B was investigated, providing ^{10}B enrichment in the investigated tissues. Quantitative imaging of ^{10}B by means of LA-ICP-MS was demonstrated as a new option to characterise the efficacy of boron compounds for BNCT.

Keywords Laser ablation-inductively coupled plasma-mass spectrometry (LA-ICP-MS) · Boron neutron capture therapy (BNCT) · Tissue sections · Quantification

Published in the topical collection *Spectrochemical Plasmas for Clinical and Biochemical Analysis* with guest editors Alfredo Sanz-Medel and María Montes Bayón.

Olga Reifschneider and Christian L. Schütz contributed equally to this work.

O. Reifschneider · M. Sperling · U. Karst (✉)
Institute of Inorganic and Analytical Chemistry, University of Münster, Corrensstrasse 30, 48149 Münster, Germany
e-mail: uk@uni-muenster.de

C. L. Schütz · G. Hampel · T. Ross
Institute of Nuclear Chemistry, University of Mainz, Fritz-Strassmann-Weg 2, 55099 Mainz, Germany

C. Brochhausen
Institute of Pathology, University of Mainz, Langenbeckstrasse 1, 55131 Mainz, Germany

M. Sperling
European Virtual Institute for Speciation Analysis (EVISA), Mendelstr. 11, 48149 Münster, Germany

Introduction

Qualitative and quantitative boron analysis is important in a variety of fields. There are two naturally occurring stable isotopes, ^{10}B and ^{11}B, with abundances of 19.9 and 80.1 %, respectively.

As boron is considered to be an essential element for plants and humans [1, 2], but also toxic above certain concentration levels [3], reliable methods for boron analysis in biological samples are required. This is particularly important in the case of boron neutron capture therapy (BNCT) of various types of cancer, which relies on the nuclear reaction that occurs when ^{10}B captures a thermal neutron. The formed unstable ^{11}B* nucleus undergoes instantaneous nuclear fission to yield an alpha particle and a ^{7}Li nucleus (^{10}B(n,α)^{7}Li) [4]. Since these species are characterised by high linear energy transfer (LET) and a very short range (<10 μm) in tissues, selective delivery of a high radiation dose to cells containing a certain amount of ^{10}B is possible [5]. The selective delivery of ^{10}B to tumour cells is facilitated by compounds with specific targeting abilities and an enrichment of the ^{10}B isotope to 99.9 %.

The radiation dose is proportional to the boron concentration in cells and tissues [6]. Therefore, in clinical applications as well as in preclinical research, the precise and accurate boron determination in blood samples, tissues and cells is mandatory. The techniques most frequently relied on in BNCT are also very commonly used for boron analysis in

inorganic matrices [7], namely inductively coupled plasma-mass spectrometry (ICP-MS), inductively coupled plasma-optical emission spectroscopy (ICP-OES) and prompt gamma activation analysis (PGAA) [8–12]. While ICP-MS and ICP-OES both require sample digestion before analysis, PGAA is a non-destructive method. Neither of the plasma spectroscopic methods can be used in its standard configuration with sample introduction by means of a nebulizer to carry out spatially resolved boron determination. For reconstruction of the local boron distribution in a sample by PGAA, two-dimensional gamma-ray detectors are required, which are not available in most facilities. However, the task of spatially resolved boron analysis in tissues is essential particularly in preclinical BNCT research. In clinical applications, most analyses are carried out based on blood samples.

The local boron distribution is of particular interest if the efficacy of a boron compound is tested, e.g., to assess the uptake in specific cells and tissues or the pharmacokinetic distribution over a period of time. For the analysis of pharmacokinetics in vivo and for treatment planning, positron emission tomography (PET) [13] or magnetic resonance imaging (MRI) [14] have been used in recent years. To study biological materials from biopsies or in vitro samples, other qualitative, semi-quantitative and quantitative techniques with higher resolution have been tested and applied, including electron energy loss spectroscopy (EELS) [15], sputter-initiated resonance ionisation microprobe (SIRIMP) or laser atomization resonance ionisation microprobe (LARIMP) [16] and, most notably, secondary ion mass spectrometry (SIMS) [17–20].

However, many of these methods require time consuming and complicated sample preparation, as well as long periods of time for the analysis and are therefore not ideally suited for high sample throughput or for a complete scan of an entire tissue section. A method requiring very simple sample preparation and allowing both qualitative and quantitative analysis of the ^{10}B distribution is high resolution quantitative autoradiography [21] or quantitative neutron capture radiography (QNCR) [22–25], which allows imaging of boron by recording the fission fragments of the ($^{10}B(n,\alpha)^{7}Li$) reaction with solid state nuclear track detectors (SSNTD). By use of suitable reference materials, quantitative boron analysis is possible as well. Depending on the analytical protocol, both imaging and quantification can be carried out on a cellular scale. With neutron radiographic methods, the complete imaging of a greater number of tissue sections is easily possible. However, for analysis, a strong, suitable neutron source is required, usually a nuclear reactor or a particle accelerator, which are not easily available.

In the past, ICP-MS analysis in combination with laser ablation has emerged as a very reliable technique for surface analysis of different materials. This method uses a focused laser beam for vaporization of solid sample material, which is then transported to the inductively coupled plasma of an ICP-MS instrument using argon or helium as carrier gas (LA-ICP-MS). It is a very reliable method in terms of low matrix effects and low formation rates of polyatomic interferences and is used, e.g., for the determination of isotope variation in nature or age dating and for a number of applications in the nuclear industry [26, 27]. Additionally, LA-ICP-MS has been successfully applied for the analysis of elements in biological samples including tissues [28–31]. However, for quantification of various elements in tissues, certified reference materials (CRM) are rarely available. Different strategies for calibration have been published, e.g., based on liquid solutions [32] or using tissue for the production of matrix-matched standards [33–35]. The latter approach [25, 35] has already been adapted for the quantification of metallodrugs (Pt), MRI contrast agents (Gd) and Sr in different tissues such as in heart, rib, brain and tumour tissue sections by means of LA-ICP-MS [29].

In this work, a method for quantitative ^{10}B bioimaging by LA-ICP-MS and matrix-matched standards is developed and applied to support BNCT.

Material and methods

Samples

Samples analysed in this study were collected during a preclinical trial (EudraCT number 2006-002796-40) to investigate the uptake behaviour of *p*-boronophenylalanine-fructose (BPA-f) in cancerous lesions and tumour-free tissue of the liver. BPA (Hammercap/Syntagon, Sweden) contained ^{10}B enriched to 99.9 % isotopic purity. Before infusion, BPA was complexed with fructose to increase solubility in blood.

Patients undergoing typical removal of one liver lobe (hemihepatectomy) because of colorectal liver metastases were included in the study. During surgery, ^{10}B was administered to each patient by an intravenous infusion of 200 mg/kg body weight of BPA-f for 2 h. During this time, the liver specimen was surgically removed and an ex situ perfusion using histidine-tryptophan-ketoglutarate (HTK) solution was started immediately. A 2.0-L HTK solution via the portal vein and 0.5 L via the hepatic artery were used. This protocol was chosen in order to reach a degree of resemblance to the approach required for future clinical use with total hepatectomy, ex situ BNCT and re-implantation of the liver after neutron irradiation. Further details about patients and aims of the study can be found elsewhere [11, 25].

The identity of the biopsies was confirmed by a pathologist before proceeding to sample preparation, e.g., the production of cryosections with a microtome. From the tissue biopsies fixed with TissueTek, which is a mixture of water soluble glycols and resins, a series of cryosections was cut for neutron radiographic as well as histomorphological analysis and subsequently transferred on glass slides. These were free of

boron, as confirmed by neutron capture radiography performed at the TRIGA research reactor of the Institute of Nuclear Chemistry in Mainz. The remainder of the blocks was used for further analysis [18]. The cryosections were stored at −20ºC to avoid contamination or redistribution of boron within the sample. Optical images were recorded using a Zeiss Axioplan microscope at a magnification of ×200 and a Zeiss Axio Cam (Carl Zeiss, Oberkochen, Germany), a reflex camera equipped with a 8.2 Mio. CCD chip. Image analysis was performed using MATLAB (The MathWorks, Version 7.5.0.338 (R2007b)).

Preparation of calibration standards

Calibration standards were originally prepared for QNCR [24], which suffers from the lack of a suitable CRM as well. The protocol for the production of calibration standards was first described elsewhere [30, 35]. A slurry of whole blood with BPA-f as boron compound with concentrations between 0.1 and 200 μg/g ^{10}B was selected as matrix-equivalent material. For analysis by QNCR, the use of whole blood was not problematic, because matrix effects occur in the emission and subsequent attenuation of charged particles upon neutron capture, e.g., protons (^{14}N(n,p)^{14}C). With respect to this effect, homogenised tissue and whole blood show similar characteristics. Regarding the elemental composition, dried and therefore solid whole blood is suitable for matrix-matched calibration using LA-ICP-MS.

As support, carboxymethyl cellulose solution produced from carboxymethyl cellulose sodium salt with water was frozen by immersion in liquid nitrogen in a specially designed and fabricated open box to form a solid, rectangular block. While the walls of the box were designed as flexible frame, which could be removed and attached independently, the bottom of the box was designed to also serve as holder of the block for cutting with the microtome. The block was left overnight at −20 °C to ensure complete solidification. The next day, a series of holes was drilled into the block, one for each boron concentration of the prepared slurry. The slurry was then filled into the holes and left for freezing for 2 h. Single slices were cut in a whole-body cryomicrotome (PVM, Stockholm, Sweden) from the block using adhesive, boron-free polyvinyl chloride tape to pick up the slice and then freeze-dried overnight. A very similar method for the production of calibration standards has recently been published by Pugh et al. [30].

Analysis by LA-ICP-MS

For quantitative imaging of boron in cancerous and tumour-free tissue after BNCT, a laser ablation model LSX 213 (CETAC Technologies, Omaha, NE, USA) with a standard cylindrical ablation cell (25 cm^3 effective volume) was coupled to a quadrupole-based ICP-MS system (iCAP Qc, Thermo Fisher Scientific, Bremen, Germany) by means of a Tygon tubing. The dry aerosol from the laser ablation unit was directly introduced into the injector pipe of the ICP-MS. Because of improved washout characteristics in the ablation chamber, helium (0.7 L/min) was utilized as carrier gas. After the sample outlet, argon was added to ensure good plasma stability (0.8 L/min). The laser parameters such as laser energy, frequency and scan rate were optimized to receive quantitative ablation of the sample material. The tissue was ablated using a multiline scan method without gap between the lines with a spot size and a scan rate of 50 μm and 50 μm s^{-1}, respectively. The laser was operated at a shot repetition rate of 20 Hz and the averaged output energy of 2.34 mJ/shot.

The setup was tuned daily for maximum intensity and low levels of oxides and doubly charged ions using a fully automated approach optimizing parameters like position of the torch, extraction voltage and the additional carrier gas flow of argon as well as the most relevant ion lenses in front of the mass analyser. The oxide ratio (^{232}Th^{16}O$^+$/^{232}Th$^+$, *m/z* 248/232 ratio) as well as the doubly charged ion ratio (^{137}Ba^{++}/^{137}Ba$^+$, *m/z* 68.5/137.0 ratio) was maintained below 1 % during ablation of the standard reference material NIST 612 (trace elements in glass, National Institute of Standards and Technology, Gaithersburg, MD, USA). The ICP-MS conditions were set to RF power 1,550 W and auxiliary gas flow rate 0.8 L min^{-1}. ^{10}B and ^{11}B were monitored with 0.25 s dwell time and one channel for each isotope. During all experiments, nickel sampler and skimmer without insert and a quartz injector pipe with an inner diameter of 3.5 mm were installed in the interface of the ICP-MS. The analysis was performed in standard mode of the ICP-MS instrument.

The prepared standard sections with 50 μm thickness were ablated using the same parameters with six lines of 5 mm length (100 s ablation time) per section. Calibration data were obtained by linear regression of the average signal intensities of each standard. The calibration function was then used to convert all pixels from ^{10}B signal intensities to concentrations in micrograms per gram. Image processing was carried out using Origin 8.0 (Originlab Corporations, Northampton, MA, USA) and ImageJ (National Institute of Health, Bethesda, MD, USA) to convert the transient signals into color-coded 2D distribution maps.

Results and discussion

Calibration by means of matrix-matched standards

For therapy planning, spatially resolved quantitative data about the enrichment of the utilized ^{10}B compound are essential. For this purpose, the ^{10}B content was determined at

50 μm spatial resolution using matrix-matched standards based on whole blood. According to Pugh et al., the standard preparation procedure is suitable for the quantification of metallodrugs (Pt) and MRI contrast agents (Gd) in heart, rib, brain and tumour tissue sections by means of LA-ICP-MS. However, the method has not yet been used for boron and for isotope enriched samples. In this study, the spiking of whole blood was performed using ^{10}B enriched BPA-f, which is applied in BNCT. Previously, the ^{10}B concentration of the matrix-matched standards was confirmed by Prompt Gamma Activation analysis, showing good recovery rates of 100.1±6.9 %. The imaging study by means of LA-ICP-MS was performed 2 years after the preparation of standards. The standard sections were prepared with the same thickness such as the liver samples (50 μm) and quantitatively ablated immediately prior to tissue samples. The laser parameters were optimized for quantitative ablation of the liver sections without penetration of the glass slide to avoid fractionation effects during ablation, transport and ionisation in the ICP. Similar ablation behaviour was observed with respect to the microscopic evaluation of the ablated areas and craters of standards and liver tissue slices. A good linearity with a correlation coefficient of R^2=0.999 was achieved within the selected concentration range between 0.2 and 212.5 μg/g including ten calibration points. The obtained calibration curve is shown in Fig. 1. Using this method, low limits of detection and quantification (LOD, LOQ), according to the 3σ and 10σ criteria of 5 and 17 ng g^{-1}, respectively, for ^{10}B, were achieved. Despite the long-term storage of the blood-based standards, the quality was not impaired according to the calibration results presented in this section.

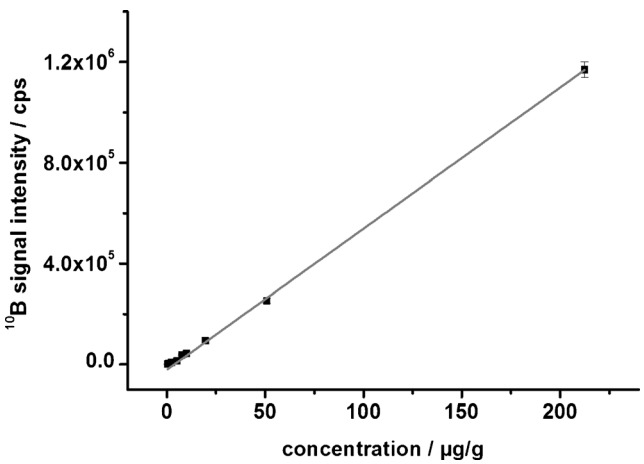

Fig. 1 Calibration curve obtained by ablation of matrix-matched standards based on blood spiked with different amounts of ^{10}B-enriched BPA-f

Imaging of ^{10}B and ^{11}B in liver sections by means of LA-ICP-MS

Cancerous and tumour-free tissues from human liver surgically removed after BNCT were prepared as slices of 50 μm thickness to investigate the uptake behaviour of *p*-boronophenylalanine-fructose (BPA-f). In Fig. 2a, the bright field micrograph of the investigated tumour tissue with dimensions of 7.7 mm×8.7 mm is observed. The tissue structure is mostly heterogeneous, which is characteristic for this type of metastasis, as they contain, for example, much fibrotic tissue. The tissue was collected in a clinical phase I study (EudraCT number: 2006-002796-40) to assess the pharmacokinetics and pharmacodynamics of BPA-f in colorectal liver metastases. The study protocol required the perfusion of the tissue specimen after surgery to remove all blood containing boron from the blood vessels in order to not compromise future boron analysis in tissue.

Using LA-ICP-MS, distribution maps of both boron isotopes were generated with 50-μm spot size. Figure 2b shows transient signals of a single line scan of 150 s (7.5 mm line length) for ^{10}B and ^{11}B in the cancerous tissue section. Signal intensities of ^{10}B (up to 10^5 cps) and ^{11}B (up to $2\cdot10^3$ cps) were observed depending on the position on the tissue. With respect to the natural abundance of both boron isotopes, a high uptake of ^{10}B is observed. The concentration data of ^{10}B were combined in quantitative images with 50 μm resolution as shown in Fig. 2c. The image reveals spots with rather high boron concentrations up to 47 μg g^{-1}, of which some represent inclusions of BPA-containing blood (Fig. 2c white arrows) that was not completely flushed out through perfusion. Therefore, the cavities in which these boron concentrations were found are sections through blood vessels. The difference between areas in the tissue of distances of only several tens of micrometers (=several cell diameters) amounts up to a factor of 2. However, the boron concentration appears to be still quite homogeneous. This is mostly due to the fact that fibrotic tissue shows similar boron levels as the neighboring cancerous cells [24]. Higher gradients were found in samples with larger areas containing necrotic cells, however, these are not present in the sample shown in this paper. The average concentration throughout the ablated area is 7.3 μg g^{-1} with a SD=3 μg g^{-1} excluding the hotspots, which is slightly lower than measured by QNCR: 9.9 μg g^{-1} (mean), with SD= 4.0 μg g^{-1} and a range of 7.7–17.5 μg g^{-1}. It should be emphasized at this point that the number of the investigated pixels per single image in case of the QNCR was limited to 2,600×2,060, representing an

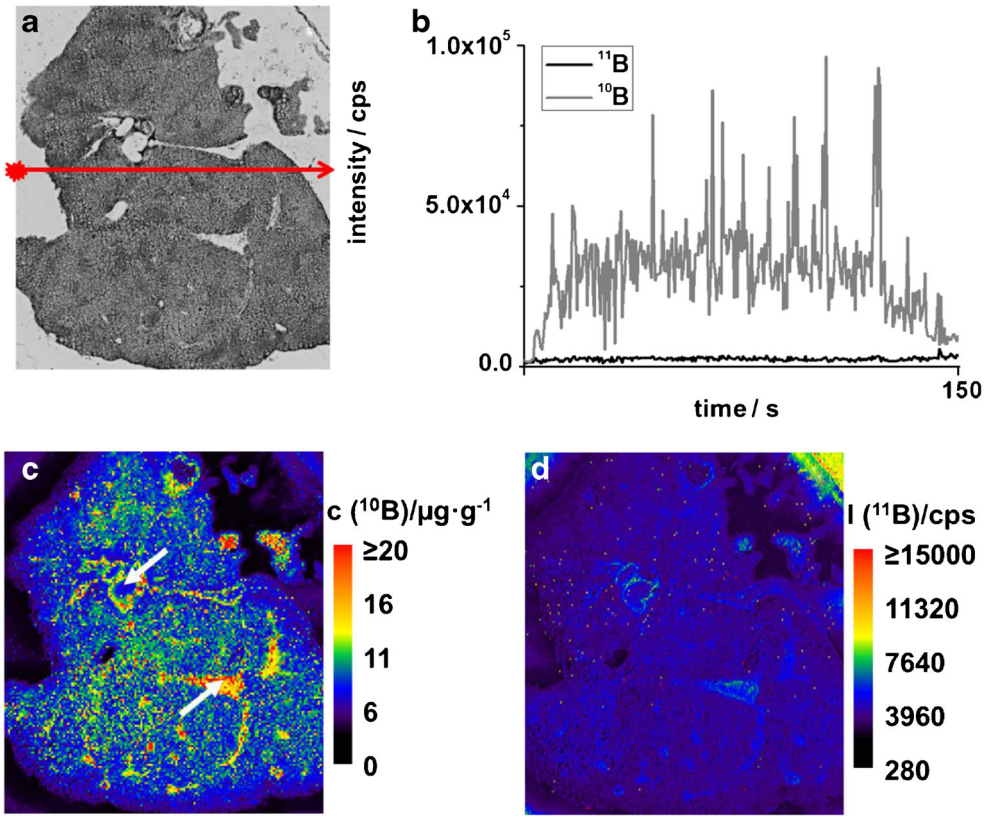

Fig. 2 **a** Bright field micrograph of the investigated section of a liver tumour obtained from a human patient after BNCT; **b** transient signals of ^{10}B and ^{11}B of a single line scan marked in **a**, the enrichment of ^{10}B in the tissue is observable; **c** the corresponding quantitative ^{10}B distribution with a concentration range 0–20 µg g^{-1}; **d** the qualitative ^{11}B distribution at 50 µm resolution

area of 410×325 μm^2 and only selected areas (8–15 single images) were analysed per tissue section, whereas using LA-ICP-MS, every spot of the tissue surface was included by linewise ablation without any gap between the lines. Furthermore, this patient continuously lost considerable amounts of blood during surgery and infusion. Therefore, blood transfusions were required during the same period of time as the BPA infusion. As a result, an expected saturation of at least 20 ppm ^{10}B in the tumour could not be reached during the infusion time. The absolute boron levels of the specific samples presented in this manuscript are therefore not directly comparable. A more detailed evaluation of all samples obtained and analysed during the study and the subsequent clinical implications of the findings have been published elsewhere [11, 25].

With respect to the distribution map of ^{10}B in tumour-free tissue (Fig. 3b), similar results are obtained. The maximum and average concentrations are 51 and 7.6 µg g^{-1} (mean), with SD=4.4 µg g^{-1} respectively. Quantitative radiography findings were slightly lower than for LA-ICP-MS, but still in agreement: 7.6 µg g^{-1} (mean), with SD=2.0 µg g^{-1} and a range of 5.1–8.8 µg g^{-1} (excluding the hot spots). The distribution of boron is quite homogeneous in this sample as well. However, it should be noted that this sample was retrieved from another patient than the one shown in Fig. 2a–d. In all non-cancerous tissue collected during the study, i.e. liver tissue, the homogeneity was confirmed histomorphologically, unless steatosis was present, which was hardly the case in the example shown here. Primary liver cells (hepatocytes) may retain lipids due to an impairment of the triglyceride metabolism; such cells are called steatotic [24]. Because of the cryopreparation, the tissue is enclosed by the transparent embedding medium (TissueTek). This area is barely visible in the optical micrographs in Fig. 2a, showing a high boron background in the upper left and right corner of the ^{10}B distribution in Fig. 2c.

$^{10}B/^{11}B$ isotope ratio in liver samples after infusion of BPA-f

With regard to the very similar ionisation behaviour of both boron isotopes in the argon plasma of the ICP-MS instrument, the isotope ratios can be calculated using the signal intensities. Due to possible mass bias effects inherent for the quadrupole-based ICP-MS used for this study, only approximate values can be calculated [35]. To elucidate the enrichment, $I(^{10}B)/I(^{11}B)$ ratio images were generated according to the absolute intensities of

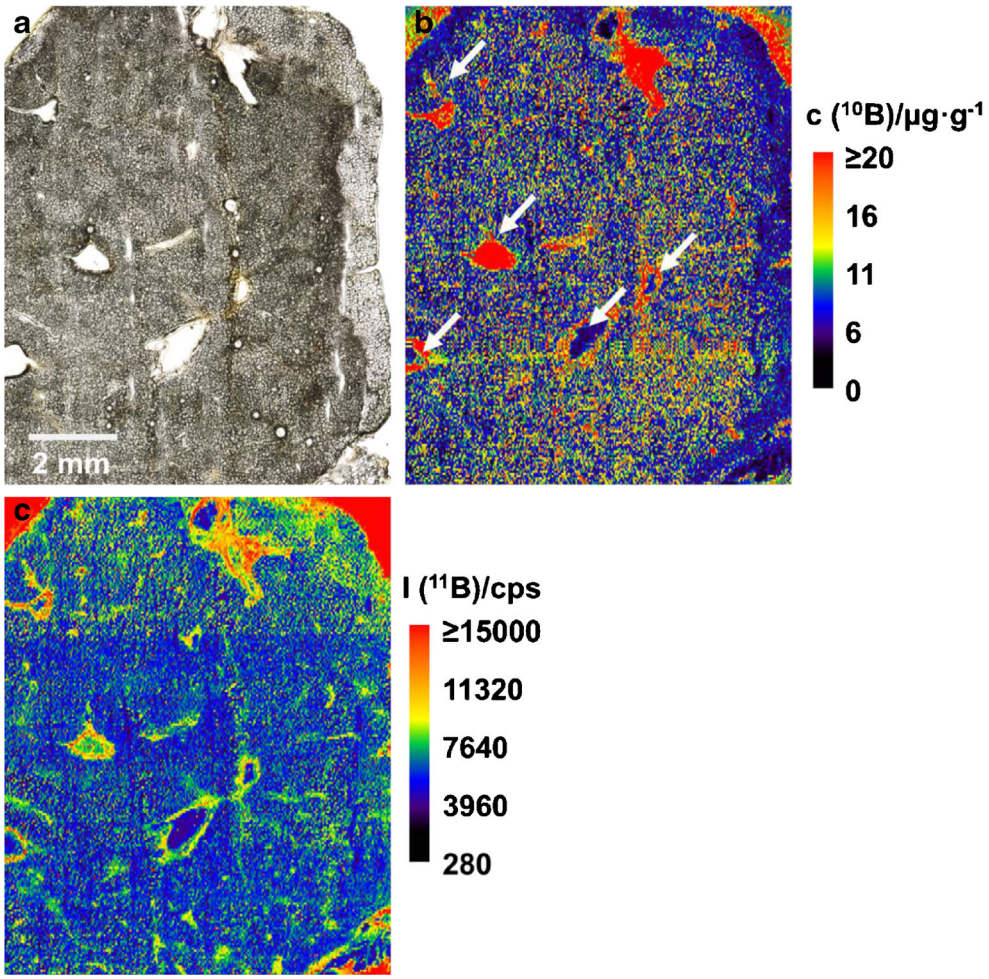

Fig. 3 **a** Bright field micrograph of the investigated section of tumour-free liver area obtained from a human patient after BNCT; **b** the corresponding quantitative ^{10}B distribution with a concentration range 0–20 µg g^{-1}; **c** the qualitative ^{11}B distribution at 50 µm resolution

both isotopes. The images are shown for cancerous and tumour-free tissue in Fig. 4a, b, respectively. In both cases, the $^{10}B/^{11}B$ ratio throughout the tissue shows high values of up to 76 in cancerous tissue (Fig. 4a) and 104 in tumour-free tissue (Fig. 4b). By means of these images, the high enrichment grade of ^{10}B in the liver tissue can be visualized. Nominally, the enrichment of $^{10}B/^{11}B$ is 99.9 %.

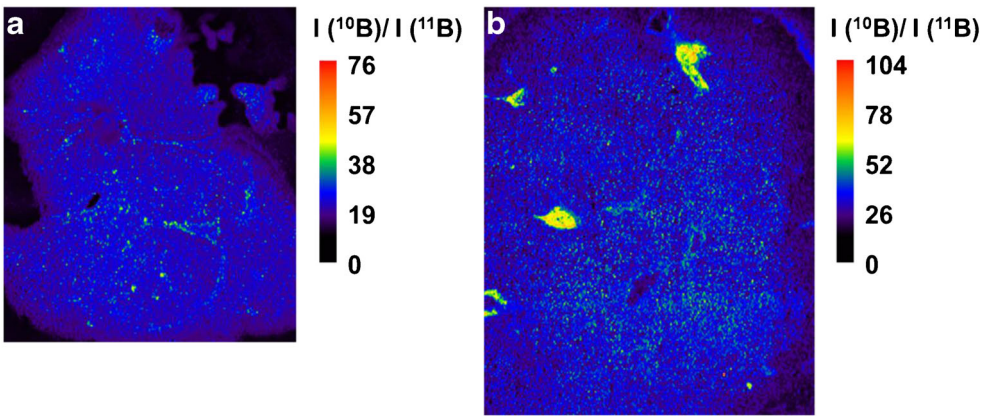

Fig. 4 **a** I(^{10}B)/I(^{11}B) ratio in the tumour section; **b** I(^{10}B)/I(^{11}B) ratio in the tumour-free section

Conclusions

In this work, an alternative method to QNCR and PGAA to investigate ^{10}B distribution in human tumour and tumour-free tissue after application of boron compounds for BNCT based on quantitative elemental bioimaging by means of LA-ICP-MS was developed. Using this method, a limit of detection of 5 ng g^{-1} together with a high spatial resolution of 50 μm was achieved. External calibration using ^{10}B isotope-enriched BPA-f standards based on whole blood, which were proved to be suitable for QNCR analysis as well, showed precise quantification results. The distribution in cancerous and healthy tissue was investigated using the given calibration method showing an enrichment of ^{10}B in both kinds of tissue. The quantitative distribution data determined with the LA-ICP-MS method are in good agreement with the data from the radiographic analysis. The developed method is showing better resolution (50 μm) using a relatively simple setup in comparison with QNCR.

Acknowledgments Parts of this study were supported by the Cells in Motion Cluster of Excellence (CiM-EXC 1003), Münster, Germany (project FF-2013-17). The contribution of Christian L. Schütz was generously supported by a grant provided by the Boehringer Ingelheim Foundation (Ingelheim, Germany).

References

1. Nielsen FH (1996) J Trace Elem Exp Med 9:215
2. Nielsen FH (2000) Nutrition 16:512–514
3. Başaran N, Duydu Y, Bolt HM (2012) J Trace Elem Med Biol 26: 165–167
4. Barth RF, Vicente MGH, Harling OK, Kiger WS, Riley KJ, Binns PJ, Wagner FM, Suzuki M, Aihara T, Kato I, Kawabata S (2012) Radiat Oncol 7:146
5. Coderre JA, Morris GM (1999) Radiat Res 151:1–18
6. Lu X-Q, Kiger WS (2009) Radiat Res 171:646–656
7. Tonarini S, Pennisi M, Adorni-Braccesi A, Dini A, Ferrara G, Gonfiantini R, Wiedenbeck M, Goning M (2003) Geostand Newslett 27:21–39
8. Nyomora AMS, Sah RN, Brown PH, Miller RO (1997) Fresenius J Anal Chem 357:1185–1191
9. Linko S, Revitzer H, Zilliacus R, Kortesniemi M, Kouri M, Savolainen S (2008) Scand J Clin Lab Inv 68:696–702
10. Probst TU, Berryman NG, Lemmen P, Weissfloch L, Auberger T, Gabel D, Carlsson J, Larsson B (1997) J Anal Atom Spectrom 12:1115–1122
11. Schmitz T, Appelman K, Kudejova P, Schütz C, Kratz JV, Moss R, Otto G, Hampel G (2011) Appl Radiat Isotopes 69:936–941
12. Schütz CL, Brochhausen C, Hampel G, Iffland D, Kuczewski B, Otto G, Schmitz T, Stieghorst C, Kratz JV (2012) Anal Bioanal Chem 404: 1887–1895
13. Evangelista L, Jori G, Martini D, Sotti G (2013) Appl Radiat Isotopes 74:91–101
14. Porcari P, Capuani S, D'Amore E, Lecce M, La Bella A, Fasano F, Migneco LM, Campanella R, Maraviglia B, Pastore FS (2008) Phys Med Biol 53:6979–6989
15. Michel J, Sauerwein W, Wittig A, Balossier G, Zierold K (2003) J Microsc 210:25–34
16. Arlinghaus HF, Spaar MT, Switzer RC, Kabalka GW (1997) Anal Chem 69:3169–3176
17. Chandra S, Tjarks W, Lorey DR, Barth RF (2008) J Microsc 229:92–103
18. Chandra S, Barth RF, Haider S, Yang W, Huo T, Shaikh AL, Kabalka GW (2013) Biodistribution and subcellular localization of an unnatural boron-containing amino acid (Cis-ABCPC) by imaging secondary ion mass spectrometry for neutron capture therapy of melanomas and gliomas. PLoS ONE 8:1–9
19. Marchetti I, Menichetti L, Kusmic C, de las Heras LA, Salvadori P, Fuoco R, Belloni F, ĹAbbate A, Betti M (2009) Spectrochim Acta B 64:911–920
20. Yokoyama K, Miyatake S-I, Kajimoto Y, Kawabata S, Doi A, Yoshida T, Okabe M, Kirihata M, Ono K, Kuroiwa T (2007) Radiat Res 167:102–109
21. Kiger WS, Micca PL, Morris GM, Coderre JA (2002) Radiat Prot Dosim 99:409–412
22. Bortolussi S, Pinto JM, Thorp SI, Farias RO, Soto MS, Sztejnberg M, Pozzi ECC, Gonzalez SJ, Gadan MA, Bellino AN, Quintana J, Altieri S, Miller M (2001) Appl Radiat Isotopes 69:1924–1927
23. Portu A, Carpano M, Dagrosa A, Nievas S, Pozzi E, Thorp S, Cabrini R, Liberman S, Saint Martin G (2011) Appl Radiat Isotopes 69: 1698–1701
24. Portu A, Carpano M, Dagrosa A, Cabrini RL, Saint Martin G (2013) Biotech Histochem 88:217–221
25. Schütz C, Brochhausen C, Altieri S, Bartholomew K, Bortolussi S, Enzmann F, Gabel D, Hampel G, Kirkpatrick CJ, Kratz JV, Minouchehr S, Schmidberger H, Otto G (2011) Radiat Res 176: 388–396
26. Becker JS, Dietze H-J (2000) Fresen J Anal Chem 368:23–30
27. Pisonero J, Fernández B, Günther D (2009) J Anal Atom Spectrom 24:1145–1160
28. Ghazi AM, Wataha J, O'Dell N, Singh B, Simmons R, Shuttleworth S (2002) J Anal Atom Spectrom 17:1295–1299
29. Becker JS, Zoriy M, Matusch A, Wu B, Salber D, Palm C, Becker JS (2010) Mass Spectrom Rev 29:156–175
30. Pugh JAT, Cox AG, McLeod CW, Bunch J, Whitby B, Gordon B, Kalber T, White E (2011) J Anal Atom Spectrom 26:1667–1673
31. Reifschneider O, Wehe CA, Diebold K, Becker C, Sperling M, Karst U (2013) J Anal Atom Spectrom 28:989–993
32. Becker JS, Zoriy MV, Pickhardt C, Palomero-Gallagher N, Zilles K (2005) Anal Chem 77:3208–3216
33. Zoriy MV, Dehnhardt M, Matusch A, Becker JS (2008) Spectrochim Acta B 63:375–382
34. Reifschneider O, Wehe CA, Raj I, Ehmcke J, Ciarimboli G, Sperling M, Karst U (2013) Metallomics 5:1440–1447
35. Gabel D, Holstein H, Larsson B, Gille L, Ericson G, Sacker D, Som P, Fairchild RG (1987) Cancer Res 47:5451–5454